

Petrological and geochronological constraints on the origin of the Palimé–Amlamé granitoids (South Togo, West Africa): A segment of the West African Craton Paleoproterozoic margin reactivated during the Pan-African collision

Y. Agbossoumondé^a, R.-P. Ménot^{b,*}, J.L. Paquette^c, S. Guillot^d, S. Yéssoufou^e, C. Perrache^b

^a *Département des Sciences de la Terre, Université de Lomé, BP 1515, Lomé, Togo*

^b *Université Jean Monnet, CNRS - UMR 6524, Magmas et Volcans, 23, rue Dr. P. Michelon, 42023 - Saint Etienne Cedex 02, France*

^c *Université Blaise Pascal, CNRS - UMR 6524, Magmas et Volcans, 5, rue Kessler, 63038-Clermond-Ferrand cedex, France*

^d *Université Joseph Fourier, CNRS - UMR 5025, Laboratoire de Géodynamique des Chaînes Alpines, 1381, rue de la Piscine, 38400 St Martin d'Hères, France*

^e *Département des Sciences de la Terre, Université d'Abomey-Calavi, FAST, 01 BP 526 Cotonou, Bénin*

Received 8 February 2006; received in revised form 9 November 2006; accepted 29 January 2007

Available online 9 February 2007

Abstract

The Palimé–Amlamé Pluton (PAP) in southern Togo, consists of silica-rich to intermediate granitoids including enclaves of mafic igneous rocks and of gneisses. They are commonly called the “anatectic complex of Palimé–Amlamé” and without any convincing data, they were interpreted either as synkinematic Pan-African granitoids or as reworked pre Pan-African plutons. New field and petrological observations, mineral and whole-rock chemical analyses together with U–Pb zircon dating, have been performed to evaluate the geodynamic significance of the PAP within the Pan-African orogenic belt. With regard to these new data, the granitoids and related enclaves probably result from mixing and mingling processes between mafic and silicic magmas from respectively mantle and lower crust sources. They display Mg–calc-alkaline chemical features and present some similarities with Late Archaean granites such as transitional (K-rich) TTGs and sanukitoids.

The 2127 ± 2 Ma age obtained from a precise U/Pb concordia on zircon, points out a Paleoproterozoic age for the magma crystallization and a lower intercept at 625 ± 29 Ma interpreted as rejuvenation during Pan-African tectonics and metamorphism. Based on these results, a Pan-African syn to late orogenic setting for the PAP, i.e. the so-called “anatectic complex of Palimé–Amlamé”, can be definitively ruled out. Moreover according to its location within the nappe pile and its relationships with the suture zone, the PAP probably represents a fragment of the West African Craton reactivated during the Pan-African collision.

© 2007 International Association for Gondwana Research. Published by Elsevier B.V. All rights reserved.

Keywords: Calc-alkaline granitoids; Paleoproterozoic; Pan-African orogen; U–Pb zircon age; Togo; West Africa

1. Introduction

The Pan-African belt may be followed all along the eastern margin of the West African Craton (WAC) from Algeria to Brazil. It formed during accretion of the WAC to NW Gondwana (Caby, 1989; Trompette, 2000). From the Niger river (i.e. 12°N) down to the Atlantic Coast (5°N), this belt, the so-called Dahomeyide belt, cuts across north Bénin, Togo and SE-Ghana, and extends

eastwards to SW Nigeria (Fig. 1). The Dahomeyide belt was precisely described and subdivided into six lithotectonic zones by Affaton et al. (1991). The paper presented here deals with the external zones, i.e. zones I and II, that correspond to tectonic collages of various lithologies including both metasedimentary rocks from the WAC passive margin, pre-Pan-African gneisses and granitoids of poorly known origin and mafic–ultramafic rocks corresponding to the suture zone *s.l.* (Fig. 1, Sylvain et al., 1986; Castaing et al., 1988; Affaton, 1990; Agbossoumondé et al., 2001, 2004). In this paper, we have investigated the mineralogy, chemistry and geochronology of a controversial composite

* Corresponding author. Tel.: +33 4 77 48 15 10; fax: +33 4 77 48 51 08.

E-mail address: rpmenot@orange.fr (R.-P. Ménot).

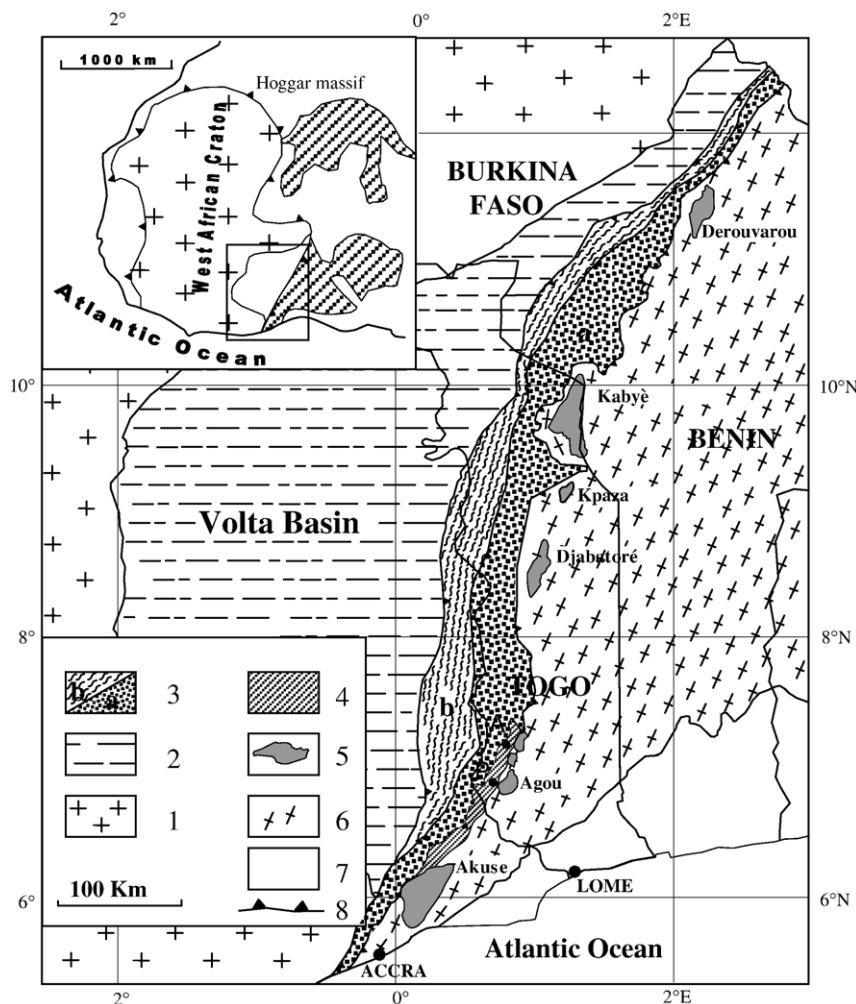


Fig. 1. Geological map with the main structural domains of Pan-African Dahomeyide Belt and location of the Palimé (P)–Amlamé (A) Pluton in SW Togo. 1: West African Craton, 2: Volta Basin, 3: Buem (b) and Atacora (a) structural units, 4: Palimé–Amlamé Pluton, 5: Ultramafic and mafic complexes, 6: Composite basement of the Benin–Nigeria unit, 7: Coastal sedimentary basin, 8: Thrust.

plutonic suite, the Palimé–Amlamé Pluton (PAP), whose age and geodynamic significance is hotly debated. For example, in one model these granitoids are thought to be part of the West African Craton reworked during the Pan-African orogeny and may be time equivalent (circa 2 Ga) of the Hô Gneiss, SE Ghana (Attoh et al., 1997; Hirdes and Davis, 2002), the Kara orthogneiss, N Togo (Affaton et al., 1991) or of the Bourré Granite, Mali (La Boisse and Lancelot, 1977; Caby and Moussine-Pouchkine, 1978). In that frame, the PAP may be considered as a tectonic window under the west vergent nappes that include Pan-African metasediments and ophiolites (Agbossoumondé et al., 2001). Alternatively, the PAP is considered as a calc-alkaline magmatic suite related to the Late Proterozoic orogenic evolution (Sylvain et al., 1986; Castaing et al., 1988). Systematic investigations have been performed on selected samples of the PAP, based on new mineral and whole rock chemistry (major, traces, REE and Sr and Nd isotopes) together with U–Pb, zircon dating. The geochemical features of the granitic rocks from the PAP have been compared to reference igneous series through chemical discrimination diagrams (e.g. Chappell and White, 1992; Pearce, 1996; Frost et al., 2001) in order to define their origin and their tectonic setting.

2. Geological environment

The PAP crops out within a peneplain bordered to the west by the spectacular cliffs of the Atacora chain and to the east by several alignments of hills scattered from Agou to Atakpame. More precisely, it forms an SSW–NNE elongated body, i.e. parallel to the regional Pan-African structural trend, within the so-called “Anatectic Complex of Palimé–Amlamé” (Fig. 1) (Sylvain et al., 1986). The granitoids are closely associated with undifferentiated gneisses and migmatites that mainly occur on the eastern part of the complex but also as enclaves of metre to 100-m size. The anatectic complex of Palimé–Amlamé is part of the regional Pan-African nappe pile (Caby, 1987; Affaton et al., 1991). It is lying upon the “Atacora unit”, i.e. the external nappes mainly built of quartzites and metapelites recrystallized in greenschists to amphibolite facies conditions (Affaton, 1990 and references therein). To the east, it is overlain by the “suture zone assemblage”, i.e. the intermediate nappes including high grade ultramafic and mafic rocks together with kyanite and phengite bearing quartzites, metapelites and various gneisses (Ménot, 1980; Ménot and Seddoh, 1985; Affaton, 1990; Attoh, 1990; Attoh et al., 1997;

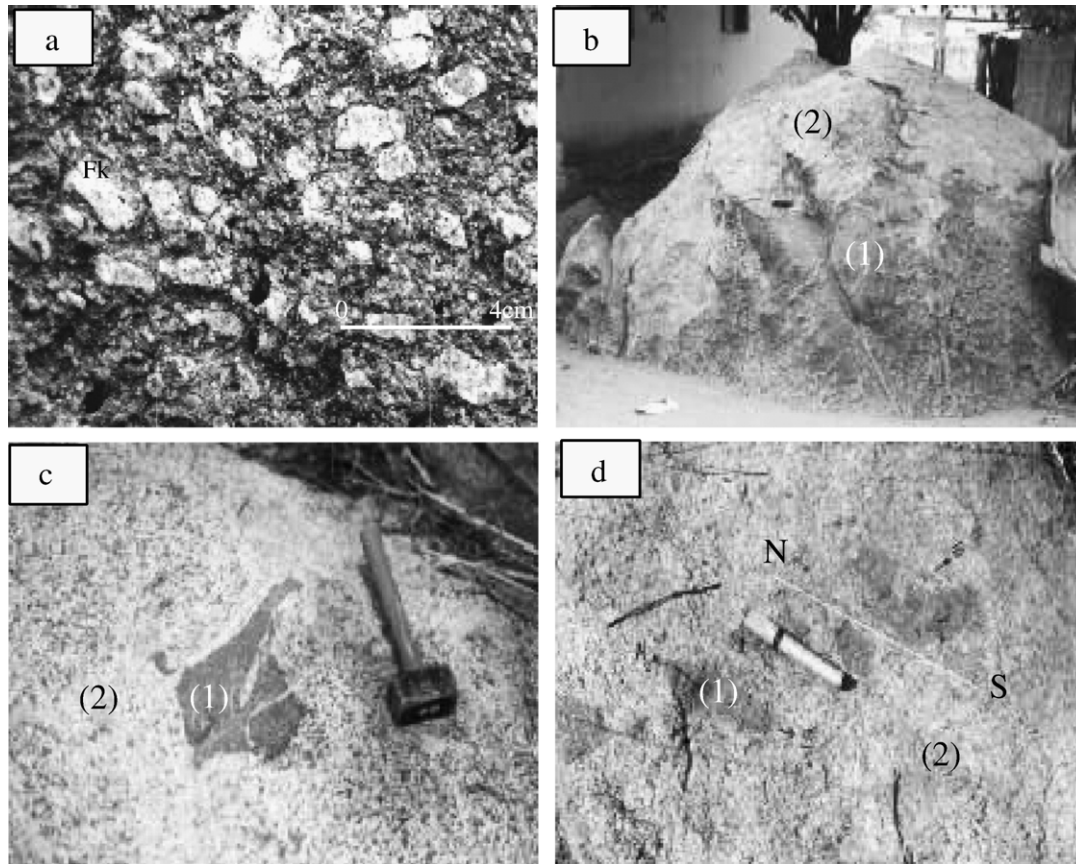


Fig. 2. Field observations on the Palimé–Amlamé Pluton. a: K-feldspar phenocrysts and magmatic fabric in monzogranites (Palimé area). b: mafic igneous enclaves (1) in isotropic monzogranites (2) (Palimé area). c: mafic igneous enclaves (1) in isotropic hornblende-rich granodiorites (2) (Amlamé area). d: metamorphic enclave (1) in granodiorites (2) (Amlamé area).

Agbossoumondé et al., 2001, 2004). The ultramafic and mafic rocks correspond to eclogites and granulites that derive respectively from oceanic crust and magmatic arc protoliths.

3. Field observations

As described by Sylvain et al. (1986), the PAP is mainly composed by two types of granitoids, biotite–muscovite and biotite–hornblende granitoids, but it also displays a number of subordinate rock types as igneous mafic enclaves, metamorphic xenoliths (migmatitic gneiss and amphibolites), aplitic and pegmatitic dykes. The petrological diversity of the PAP is also enhanced by local variations in the mineralogy and/or texture related to (i) magma–xenoliths interactions and to (ii) heterogeneous Pan-African deformation (isotropic versus gneissic facies).

The main rock types consist of: (i) biotite–muscovite monzogranite; (ii) hornblende–biotite granodiorite; (iii) hornblende rich quartz–monzodiorites. Textures vary from preserved igneous fabrics, with K-feldspar defining a strong magmatic fabric in the porphyritic samples (Fig. 2a), to strongly foliated (orthogneisses). The magmatic mafic enclaves vary from monzonite to quartz diorite compositions. They are rounded (Fig. 2b), lens-shaped or angular and brecciated (Fig. 2c) and centimetre to decimetre in size. The sharp contacts with granitoids are sometimes lobate and commonly underlined by a finer-grain size (“chilled” margin). Such features clearly indicate magma

mingling processes related to the coeval intrusion of mafic and silicic to intermediate magmas (Didier and Barbarin, 1991).

Migmatitic biotite–muscovite gneisses and subordinate amphibolites are locally abundant as country rock xenoliths of metre to 100-m size. They have been partially digested by the PAP magmas as suggested by transitional contacts and by the occurrence of hybrid rocks such as biotite–muscovite–hornblende bearing granites. The metamorphic enclaves (Fig. 2d) may be observed everywhere in the PAP, but seem to be more abundant in the southern area (Palimé).

Late aplitic to pegmatitic veins occur within the PAP rock types and consist of leucocratic muscovite bearing granites. They are generally isotropic and cut across the migmatitic gneisses. On a regional map scale, petrological heterogeneities have been distinguished within the PAP. Firstly, a southwards “differentiation” trend from mesocratic granitoids (quartz–monzodiorite, granodiorite and quartz–diorite) in the northern area (Amlamé) to more silicic and leucocratic facies (monzogranite, quartz–monzonite) in the south (Palimé). Such an evolution is consistent with statistical enrichment in mafic and metamorphic enclaves in the northern and southern parts respectively.

Secondly, with respect with structures, Pan-African deformation increases eastwards, towards the tectonic contact with the “suture zone assemblage”. Close to this contact, mylonitic orthogneisses display C/S structures and shear criteria marking out the top to the west thrusting of the “suture zone”. Regional

foliation varies from N25 to N140 in strike, generally dipping to the east (40–50°). In the western zone of the PAP, foliation may gently dip to the west. Locally, magmatic fabrics can be well preserved during Pan-African deformation but insufficient outcrops prevent the regional pattern to be precisely detailed.

4. Petrography

Based on the normative compositions, five main igneous rock types have been described within the PAP: granodiorites, monzogranite, quartz–monzonite, quartz–monzodiorite and quartz–diorite (Fig. 3).

Granodiorite (Ezm) is medium to coarse grained and porphyritic with large phenocrysts of pink K-feldspar. A greenish general color is due to both abundant hornblende and late recrystallization of plagioclase to epidote and more Na-rich feldspar. The common mineral assemblage consists of quartz–orthoclase–andesine–oligoclase–hornblende–biotite–Fe–Ti oxides–epidote–apatite and zircon. The mineralogical and textural homogeneity of sample Ezm resulted in this sample being selected for zircon dating.

Biotite monzogranites (ym22a) are medium to coarse-grained and often porphyritic. They are characterized by quartz–orthoclase–oligoclase–biotite–zircon–apatite ± hornblende ± muscovite primary assemblages. Subhedral phenocrysts of K-feldspar are commonly up to one or two centimetre long (Fig. 2a). Muscovite is always subordinate and generally restricted to contaminated facies close to country rock metamorphic enclaves.

Quartz–monzonites (ym22c) display similar magmatic mineral assemblages but with a slight depletion in quartz compared to the monzogranites (Fig. 3). A low grade metamorphic imprint is mainly related to the development of a mylonitic foliation and marked by crystallization of biotite (chlorite), muscovite, sericite, calcite, epidote, albite and quartz.

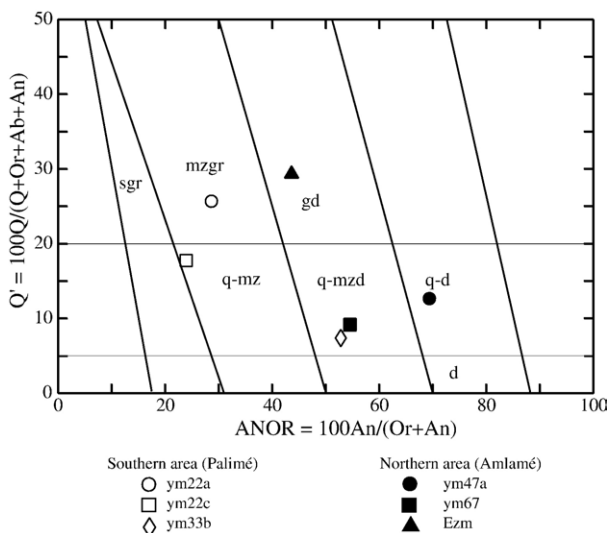


Fig. 3. Molar norm composition in a Q'-ANOR diagram after Streckeisen and Le Maitre (1979). sgr = syenogranite, mzgr = monzogranite, gd = granodiorite, q-mz = quartz–monzonite, q-mzd = quartz–monzodiorite, q-d = quartz–diorite, d = diorite.

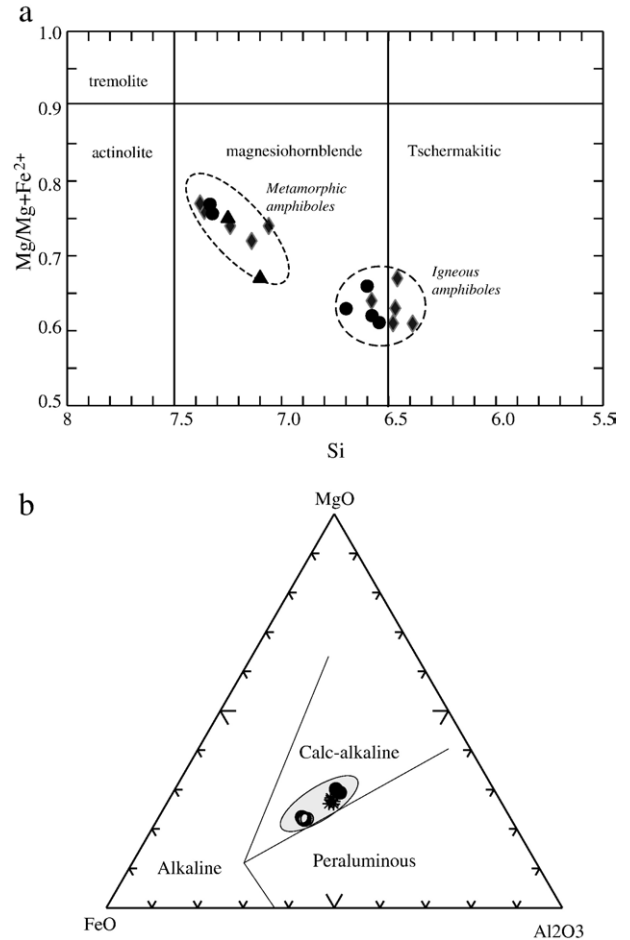


Fig. 4. a: Calcic amphiboles in samples from Amlamé area on the Leake et al. (1997) classification diagram. ▲ granodiorite (Ezm), ● quartz-diorite (ym47a), ◆ diorite (ym47b). b: composition of biotites from the Palimé–Amlamé granitoids, modified fields after Rottura et al. (1997). monzogranite O ym22a * ym34, quartz-diorite ● ym47a.

Quartz–monzodiorites (ym47a) and quartz–diorites (ym67) contain a similar mineralogical assemblage but are richer in amphibole than the granodiorites. They also display a striking porphyritic fabric with large euhedral K-feldspar crystals.

In the mesocratic granodiorites and monzodiorites, post-solidus recrystallization led to a synkinematic paragenesis of quartz, albite–oligoclase, biotite (chlorite), muscovite, pyrite, epidote and sphene. Epidote and sphene are very common and abundant in the more recrystallized facies.

Mafic igneous enclaves display quartz–monzodiorite (ym33b) to diorite compositions. Their specific host rocks are quartz–monzogranites (ym22a) and quartz–diorites (ym47a) (Table 3) from the Palimé and Amlamé areas, respectively. The mafic enclaves contain abundant green hornblende, sometimes up to 25%, andesine–oligoclase and a small amount of quartz. Biotite appears either as a late igneous mineral or as a metamorphic synkinematic phase together with abundant sphene, epidote and secondary plagioclase.

Mylonitic orthogneiss; i.e. beneath the eastern tectonic contact with the overlying suture zone assemblage and are characterized by a strong mylonitic C/S fabric with a significant enrichment in

Table 1
Representatives analyses of biotites

Samples	ym22a (monzogranite)					ym34 (monzogranite)					ym47a (quartz–diorite)			
SiO ₂	36.62	36.64	36.90	36.11	37.05	36.68	37.27	38.04	37.79	37.61	37.24	37.03	37.57	37.84
TiO ₂	1.77	1.64	1.70	1.69	1.66	1.56	1.66	2.04	2.12	1.83	1.87	1.51	1.72	1.60
Al ₂ O ₃	14.80	15.10	14.85	14.46	14.79	14.69	15.04	16.80	16.91	16.50	16.30	16.19	16.51	16.35
Cr ₂ O ₃	0.38	0.26	0.00	0.00	0.39	0.00	0.00	0.00	0.03	0.09	0.00	0.00	0.34	0.18
FeO	21.07	20.63	20.84	21.06	21.18	21.09	21.08	16.85	17.05	17.58	17.08	16.90	15.54	15.95
MnO	0.46	0.41	0.34	0.39	0.39	0.33	0.35	0.20	0.18	0.12	0.14	0.16	0.09	0.11
MgO	10.60	10.41	10.25	10.63	10.47	10.49	10.53	12.42	12.14	12.24	12.58	12.80	13.18	13.75
CaO	0.04	0.01	0.06	0.04	0.03	0.03	0.00	0.00	0.04	0.00	0.00	0.03	0.08	0.04
Na ₂ O	0.06	0.04	0.05	0.09	0.03	0.06	0.05	0.23	0.10	0.14	0.20	0.13	0.11	0.13
K ₂ O	10.30	10.30	10.06	10.05	10.14	10.22	10.15	9.88	10.39	10.02	9.83	10.08	9.57	9.97
NiO	0.02	0.00	0.01	0.01	0.01	0.00	0.00	0.03	0.00	0.02	0.20	0.01	0.00	0.01
Total	96.12	95.44	95.06	94.53	96.14	95.15	96.13	96.50	96.75	96.15	95.44	94.84	94.71	95.93
Fe ₂ O ₃ calc	0.45	0.37	0.21	0.39	0.04	0.44	0.00	0.00	0.11	0.00	0.00	0.00	0.00	0.00
FeO calc	20.66	20.28	20.64	20.70	21.14	20.69	21.08	16.85	16.94	17.58	17.08	16.89	15.54	15.95
Si	5.63	5.65	5.71	5.64	5.68	5.68	5.70	5.64	5.61	5.63	5.62	5.62	5.64	5.63
Al ^{IV}	2.36	2.34	2.28	2.35	2.31	2.31	2.29	2.35	2.38	2.36	2.37	2.37	2.35	2.36
Ti	0.20	0.19	0.19	0.19	0.19	0.18	0.19	0.22	0.23	0.20	0.21	0.17	0.19	0.17
Al ^{VI}	0.31	0.40	0.42	0.31	0.35	0.37	0.41	0.58	0.58	0.54	0.52	0.51	0.57	0.50
Cr	0.04	0.03	0.00	0.00	0.04	0.00	0.00	0.00	0.00	0.01	0.00	0.00	0.04	0.02
Fe ³⁺	0.05	0.04	0.02	0.04	0.00	0.05	0.00	0.00	0.01	0.00	0.00	0.00	0.00	0.00
Fe ²⁺	2.65	2.62	2.67	2.70	2.71	2.68	2.69	2.09	2.10	2.20	2.15	2.14	1.95	1.98
Mn	0.06	0.05	0.04	0.05	0.05	0.04	0.04	0.02	0.02	0.01	0.01	0.02	0.01	0.01
Mg	2.43	2.39	2.36	2.47	2.39	2.42	2.40	2.74	2.69	2.73	2.82	2.89	2.95	3.05
Ni	0.00	0.00	0.00	0.00	0.00	0.00	0.00	0.00	0.00	0.00	0.00	0.00	0.00	0.00
Ca	0.01	0.00	0.01	0.01	0.01	0.01	0.00	0.00	0.01	0.00	0.00	0.00	0.01	0.00
Na	0.01	0.01	0.01	0.03	0.01	0.01	0.01	0.06	0.02	0.04	0.06	0.04	0.03	0.03
K	2.02	2.02	1.98	2.00	1.98	2.02	1.98	1.87	1.97	1.91	1.89	1.95	1.83	1.89
Mg#	0.47	0.47	0.47	0.47	0.46	0.47	0.47	0.56	0.56	0.55	0.56	0.57	0.60	0.61
F	0.53	0.53	0.53	0.53	0.53	0.53	0.53	0.43	0.44	0.44	0.43	0.42	0.39	0.39
Na/Alk	0.01	0.01	0.01	0.01	0.01	0.01	0.01	0.03	0.01	0.02	0.03	0.01	0.01	0.01

secondary muscovite associated with granoblastic albite and epidote crystallization and quartz ribbons.

5. Mineral chemistry

Amphiboles occur mainly in the mesocratic granitoids from the northern PAP and in all the mafic enclaves. They both plot in the tschermakitic hornblende and Mg-hornblende fields of the Leake et al. (1997) classification (Fig. 4a), but define two distinct groups that correspond to the primary-igneous, and secondary-metamorphic, generations. The magmatic amphiboles are characterized by low Si (<6.7) and Mg# (Mg number) (<0.66) with respect to metamorphic amphiboles (Si>7.0 and Mg#>0.72). They are also richer in Fe_{tot} and Ti and display similar composition in the enclave/host granitoid pairs, as commonly observed (Ferré and Leake, 2001; Barbarin, 2004). Biotites (Table 1, Fig. 4b) increase in Fe (1.98 to 2.74) and Mn (0.01 to 0.6) and decrease in Mg# (0.61 to 0.47) from quartz–diorite (ym 47a) to monzogranite (ym22a) with constant Al^{IV} contents (2.28–2.36).

When compared to minerals of reference plutonic suites, the primary amphiboles and biotites from the PAP monzogranites, granodiorites and quartz–diorites are very similar in composition to the ferromagnesian minerals of the calc-alkaline low to high K granitoids (Ferré and Leake, 2001). Moreover, biotite plots in the calc-alkaline field according to Rottura et al. (1997) (Fig. 4b).

The total aluminum content of igneous amphiboles may be used to estimate the pressure values during magma crystallization (Schmidt, 1992; Anderson and Smith, 1995). It varies from 1.4 to 2% (Table 2) in the Tsch- to Mg-hornblendes from granodiorites (Ezm) and quartz–diorites (ym47a) and suggests a pressure of 4–6 kbar, i.e. approximate depths of crystallization of about 12–18 km. On the other hand, the hornblendes from mafic enclaves (ym47b), included in the ym47a quartz–diorite contain a maximum of 1.9 to 2.3 cation Al_{tot}, which corresponds to higher pressures of 6–8 kbar, i.e. approximate depths of 18–24 km. The contrasted values obtained on amphiboles from the enclave (ym47b)/host rock (ym47a) pair, suggest different depths of equilibration (18–24 km and 12–18 km) and successive stages of interaction between mafic and felsic magmas during ascent and emplacement. The Ti contents in secondary amphiboles (Ti=0.01–0.03) give temperature of 575 °C according to Otten (1984), and equilibrated during retrogression under amphibolite to greenschist facies conditions, which corresponds to the nappe stacking event in the Pan-African Dahomeyide orogen in southern Togo (Agbossoumondé et al., 2001).

6. Geochemistry

6.1. Major elements

The concentration of SiO₂ varies between 58.43 and 69.79 wt.%, except the mafic enclave ym33b (47%). All the

Table 2
Representative analyses of amphiboles

Samples	ym47b (diorite enclave)								ym47a (quartz–diorite)								Ezm (granodiorite)	
	Igneous amphiboles				Metamorphic amphiboles				Igneous amphiboles				Metam amphiboles		Igneous amphiboles			
SiO ₂	43.06	44.94	44.48	44.48	44.87	49.65	50.99	52.15	52.32	44.75	44.92	45.37	45.99	50.66	50.99	48.78	50.24	
TiO ₂	1.03	0.36	0.89	0.74	0.75	0.32	0.17	0.17	0.11	0.82	0.44	0.62	0.74	0.22	0.29	0.25	0.25	
Al ₂ O ₃	11.46	13.68	12.22	11.33	10.92	6.48	5.49	4.45	4.64	11.26	11.69	10.70	10.38	4.97	5.57	6.48	5.57	
Cr ₂ O ₃	0.00	0.08	0.00	0.00	0.25	0.00	0.48	0.40	0.54	0.00	0.00	0.00	0.00	0.00	0.00	0.00	0.00	
FeO	18.01	15.40	15.59	17.71	15.85	13.47	13.20	12.66	12.20	16.54	15.76	15.51	15.44	13.08	12.99	15.67	13.72	
MnO	0.19	0.28	0.28	0.23	0.25	0.29	0.33	0.43	0.39	0.13	0.17	0.18	0.12	0.33	0.33	0.38	0.33	
MgO	10.43	10.63	11.04	10.53	11.16	14.28	14.87	15.62	15.62	10.84	10.92	11.89	11.61	14.97	14.75	12.85	14.38	
CaO	11.27	10.15	11.36	11.59	11.16	12.10	12.25	12.19	11.95	11.33	11.16	11.56	11.40	11.59	11.49	11.69	11.59	
Na ₂ O	1.79	2.65	1.94	1.77	1.95	1.05	0.92	0.86	0.84	1.83	2.09	1.62	1.84	0.88	1.00	1.05	0.94	
K ₂ O	0.97	0.40	0.83	0.82	0.61	0.30	0.30	0.18	0.24	0.90	0.59	0.79	0.65	0.22	0.28	0.63	0.27	
NiO	0.00	0.02	0.00	0.06	0.03	0.01	0.01	0.02	0.01	0.04	0.00	0.00	0.00	0.00	0.00	0.00	0.00	
Total	98.21	98.59	98.63	99.26	97.80	97.95	99.01	99.13	98.85	98.47	97.74	98.24	98.17	98.99	99.77	100.30	99.62	
Fe ₂ O ₃ calc	6.27	6.88	4.65	5.86	5.22	4.28	4.27	4.71	4.63	4.69	4.46	5.56	3.87	5.06	4.50	4.99	5.05	
FeO calc	11.74	9.20	11.41	12.43	11.14	9.61	9.35	8.42	8.03	12.31	11.74	10.51	11.95	8.02	8.49	11.18	8.67	
Si	6.39	6.46	6.47	6.48	6.58	7.14	7.24	7.36	7.38	6.55	6.58	6.60	6.70	7.33	7.32	7.10	7.25	
Al ^{IV}	1.61	1.53	1.52	1.51	1.41	0.85	0.75	0.64	0.61	1.44	1.41	1.39	1.29	0.67	0.68	0.89	0.75	
Al ^{VI}	0.40	0.78	0.57	0.43	0.46	0.24	0.16	0.10	0.15	0.49	0.60	0.43	0.49	0.18	0.26	0.22	0.25	
Ti	0.11	0.03	0.09	0.08	0.08	0.03	0.01	0.01	0.01	0.09	0.04	0.06	0.08	0.02	0.03	0.02	0.03	
Cr	0.00	0.01	0.00	0.00	0.03	0.00	0.05	0.04	0.06	0.00	0.00	0.00	0.00	0.00	0.00	0.00	0.00	
Fe ³⁺	0.70	0.74	0.51	0.64	0.57	0.46	0.45	0.50	0.49	0.51	0.49	0.61	0.42	0.55	0.49	0.54	0.55	
Fe ²⁺	1.46	1.10	1.38	1.51	1.36	1.15	1.11	0.99	0.94	1.50	1.44	1.27	1.45	0.97	1.02	1.36	1.05	
Mn	0.02	0.03	0.03	0.03	0.03	0.03	0.04	0.05	0.04	0.01	0.02	0.02	0.01	0.04	0.04	0.05	0.04	
Mg	2.31	2.28	2.39	2.28	2.43	3.06	3.15	3.28	3.28	2.36	2.38	2.58	2.52	3.23	3.16	2.79	3.09	
CaB	1.79	1.56	1.77	1.81	1.75	1.86	1.86	1.84	1.81	1.77	1.75	1.80	1.78	1.80	1.77	1.82	1.79	
NaB	0.21	0.43	0.22	0.18	0.24	0.13	0.13	0.15	0.19	0.22	0.24	0.19	0.21	0.20	0.23	0.16	0.26	
K	0.18	0.07	0.15	0.15	0.11	0.05	0.05	0.03	0.04	0.17	0.11	0.14	0.12	0.04	0.05	0.11	0.04	
Mg/Mg+Fe ₂	0.61	0.67	0.63	0.61	0.64	0.72	0.74	0.76	0.77	0.61	0.62	0.66	0.63	0.77	0.76	0.67	0.75	

samples are quartz normative (Table 3). Granitoids from the northern area (Amlamé) are more mafic than that of the southern area of Palimé as shown by their higher Mg# (respectively 26–35% and 21–24%). But all the samples from the PAP correspond to magnesian granitoids (Fig. 5, Frost et al., 2001). The alumina saturation index [$A/CNK = \text{molar Al} / ((2 * \text{Ca} - 1.678\text{P}) + \text{Na} + \text{K})$] ranges from 0.76 to 1.01 indicating similarity to I-type metaluminous compositions (Fig. 6) with a slight shift to the peraluminous field (ASI close to 1) for the monzogranite sample (ym22a) from Palimé. Such a shift may be due to extreme fractionation or metapelitic country rocks assimilation (Clarke, 1992). Granitoids from the PAP are medium to high-K calc-alkaline (Fig. 7), however the K contents are lower in the samples from Amlamé than those recorded in the granitoids of Palimé. This fits quite well with mineralogical compositions dominated by abundant biotite, K-feldspar, subordinate hornblende and rare muscovite. Therefore they may be compared to I-types series (Chappell and White, 1992) and more precisely to the KCG (K-rich and K-feldspar porphyritic calc-alkaline granites) (Barbarin, 1996, 1999 and references therein).

On the Zr/TiO₂ versus SiO₂ diagram (Winchester and Floyd, 1977, Fig. 8), samples from southern and northern area (Palimé and Amlamé) plot respectively in the diorite and granodiorite fields and define a calc alkaline differentiation

trend. This is in good agreement with the normative typology (Le Maître, 1989, Fig. 3). The mafic enclave (ym33b) is gabbroic in composition (Fig. 8). All these features indicate a mixed origin with mantle and crust derived magmas and they suggest stronger country rock assimilation in southern part of the pluton (Palimé).

6.2. Trace elements

Chondrite normalized REE distribution plots (Nakamura, 1974, Fig. 9a) correspond to fractionated patterns ($\text{La}_N/\text{Yb}_N = 2.8$ to 9.1) commonly seen in calc-alkaline series rocks. However, granitoids from Palimé (southern area) display higher REE contents, more fractionated patterns ($\text{La}_N/\text{Yb}_N = 4$ to 9.14) and more significant negative Eu-anomalies ($\text{Eu}/\text{Eu}^* = 0.51$ – 0.57) than those from Amlamé (northern area) ($\text{La}_N/\text{Yb}_N = 2.8$ to 3.4; and $\text{Eu}/\text{Eu}^* = 0.95$ – 1.07) (Table 3). Such features are consistent with the more differentiated nature of the Palimé granitoids but also reflect a relative enrichment in lithophile elements (LILE), probably related to a more important crustal component.

The mafic enclave (ym33b) is characterized by higher REE contents and a distribution profile comparable to that of the host rocks (ym22). Such a geochemical similarity between mafic enclave and host rock is very common and testifies to mixing and mingling between the two magmas (Tindle, 1991).

Table 3
Major, trace-element and rare-earth element chemistry for granitoids from the PAP

Sample	Palimé area			Amlamé area		
	Qtz–monzodiorite	Qtz–monzonite	Monzogranite	Qtz–monzodiorite	Qtz–diorite	Granodiorite
	ym33b	ym22c	ym22a	ym47a	ym67	Ezm
SiO ₂	46.69	67.66	69.79	58.43	61.73	66.58
TiO ₂	1.95	0.75	0.28	0.64	0.78	0.69
Al ₂ O ₃	14.68	14.78	14.70	16.48	16.83	13.63
Fe ₂ O ₃	14.65	4.47	2.28	6.42	5.63	5.13
MnO	0.19	0.05	0.04	0.09	0.05	0.07
MgO	5.43	1.18	0.69	3.37	1.97	2.33
CaO	7.78	2.22	2.03	5.32	4.32	3.73
Na ₂ O	1.32	5.81	4.05	4.70	6.25	3.01
K ₂ O	3.57	2.96	3.98	1.47	1.78	3.15
P ₂ O ₅	0.75	0.22	0.10	0.31	0.31	0.34
LOI	1.60	0.77	0.84	1.39	0.77	0.96
Total	98.61	100.87	98.78	98.62	100.42	99.62
FeOt/(FeOt+MgO)	0.73	0.79	0.76	0.65	0.74	0.68
Mg#	0.27	0.21	0.24	0.35	0.26	0.32
ACNK = Al/((Ca - 1.678 * P) + Na + K)	0.762	0.897	1.015	0.889	0.856	0.926
Ni	34.2	2.5	6.7	30.7	8.9	20.9
Zn	225.4	71.5	36.8	97.5	74.5	77.8
Ga	28.3	17.0	17.2	21.7	21.0	17.0
Rb	79.1	78.2	100.4	24.8	33.6	57.4
Sr	827.6	471.4	431.8	764.1	880.6	660.0
Zr	586.3	660.4	152.6	151.5	206.4	279.0
Nb	17.9	17.1	4.8	3.1	4.0	2.1
Y	41.6	27.9	12.0	14.6	9.1	12.3
Hf	13.5	14.2	3.9	3.6	5.3	7.9
W	<3.0	<3.0	<3.0	<3.0	<3.0	3.6
Pb	14.9	16.4	24.8	7.8	5.7	12.7
Th	11.1	9.4	14.9	0.5	–	8.5
Ta	0.8	–	0.5	0.1	–	–
U	0.6	–	0.5	0.1	–	7.3
Sn	4.0	–	1.0	1.3	–	–
Cs	0.5	–	0.5	–	–	–
Ba	1621.0	1893.6	1146.0	1227.0	1620.1	1675.5
La	177.00	76.00	65.61	30.58	23.20	26.10
Ce	317.30	188.00	125.00	58.80	54.30	62.20
Nd	119.50	65.50	47.24	30.07	25.30	29.30
Sm	18.89	15.70	8.01	5.66	5.15	6.31
Eu	2.91	1.82	1.14	1.55	1.42	1.52
Gd	12.95	7.62	5.18	4.34	3.15	3.47
Dy	8.47	5.50	3.12	3.01	2.10	2.58
Er	3.85	2.58	1.10	1.36	0.79	1.02
Yb	3.42	1.95	0.75	1.14	0.70	0.91
Eu/Eu*	0.57	0.51	0.54	0.95	1.07	0.99
[La/Yb] _N	5.40	4.07	9.14	2.80	3.46	2.99
[Ce/Sm] _N	4.03	2.87	3.74	2.49	2.53	2.36
Q	5.4	16.7	25.0	10.9	8.3	26.7
or	25.4	18.0	24.5	9.3	10.9	19.9
ab	14.3	53.6	37.9	45.4	58.0	28.9
an	28.4	5.7	9.8	21.0	13.0	15.4
di	3.9	1.4	0.0	2.5	3.6	0.0
hy	16.1	2.7	2.0	8.7	3.8	6.9
il	0.4	0.1	0.1	0.2	0.1	0.1
ti	4.4	1.7	0.0	1.2	1.6	1.2
ap	1.9	0.5	0.2	0.7	0.7	0.8

When compared to Oceanic Ridge Granites (ORG) (Pearce et al., 1984, Fig. 9b), i.e. with granites deriving from differentiation of depleted mantle melts and devoid of any continental crust component, the PAP intrusives and the mafic igneous enclave are enriched in lithophile elements (Rb, Ba, Ce,

Th), slightly depleted in Nb and strongly depleted in Y and Yb. This implies: (i) a crustal component in the source of magmas (Leake, 1990; Tarney and Jones, 1994; Pearce, 1996); and, (ii) a garnet bearing source (Tarney and Jones, 1994), suggesting partial melting of the lower crust.

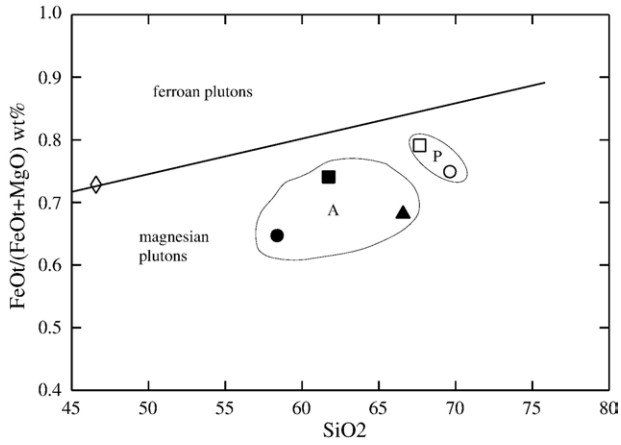


Fig. 5. FeO/(FeO+MgO) versus SiO₂ wt.% diagram after Frost et al. (2001) applied for rocks from Palimé (P) and Amlamé (A) area and showing the boundary (continuous line) between ferroan and magnesian plutons. Southern area (Palimé) O ym22a, □ ym22c, ◇ ym33b. Northern area (Amlamé) ● ym47a, ■ ym67, ▲ Ezm.

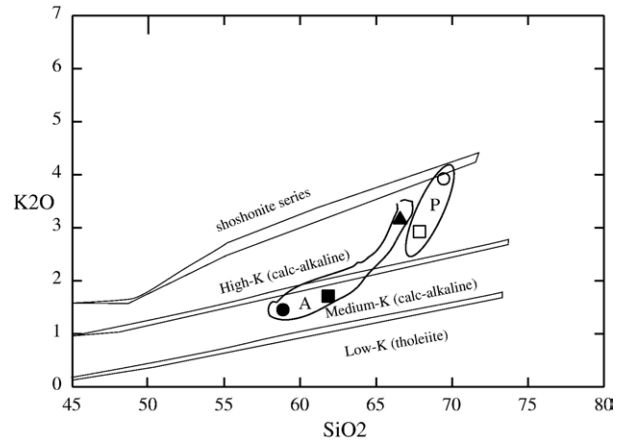


Fig. 7. Rickwood (1989) diagram showing the medium-K character for granitoids from Amlamé area and the high-K character for granitoids from Palimé area. Symbols are the same after Fig. 3. A = Amlamé, P = Palimé. Northern area (Amlamé), ● ym47a, ■ ym67, ▲ Ezm. Southern area (Palimé) O ym22a, □ ym22c.

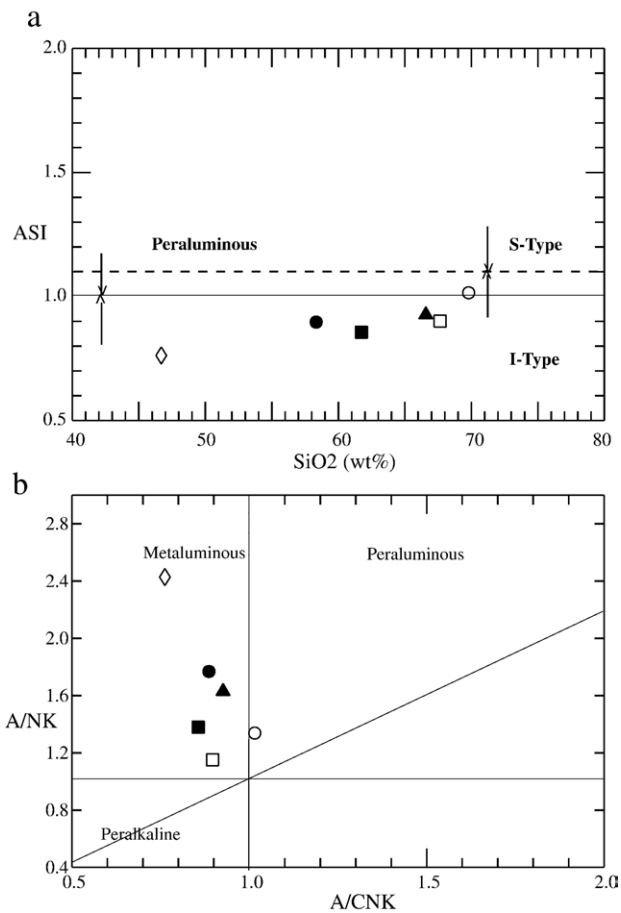


Fig. 6. Various chemical classification diagrams. (a) SiO₂-ASI diagram (Clarke, 1992) where ASI=Al/(Ca-1.678*P+Na+K). (b) A/CNK-A/NK diagram (Maniardi and Picolli, 1989), where A/CNK=molar Al₂O₃/(CaO+Na₂O+K₂O). Southern area (Palimé) O ym22a, □ ym22c, ◇ ym33b. Northern area (Amlamé), ● ym47a, ■ ym67, ▲ Ezm.

Granitoids from Amlamé area display some affinity with TTG suites (Martin, 1999; Moyen et al., 2003): they have comparable La_N/Yb_N values but positive Eu/Eu* (Table 3) and they are significantly richer in lithophile elements (Sr, K and Th). Moreover, relatively low Sr/Y (<100) ratio and Y contents (<15) characterize transitional compositions between TTG and modern arc magmatism (Defant and Drummond, 1990). More precisely, granitoids from the Amlamé area may be compared to transitional “TTGs” (Champion and Smithies, 2001, 2003) or sanukitoids (Moyen et al., 2003) and may be interpreted as magmas formed under high pressure (Y and Yb depletion) with a dominant crustal component (Champion and Smithies, 2003; Jayananda et al., 2006), i.e. by partial melting of the lowermost part of a thickened crust. This is also in good agreement with the fact that granitoids of the PAP plot in the post-collision granite field of the (Y+Nb) versus Rb diagram of Pearce (1996 – not shown).

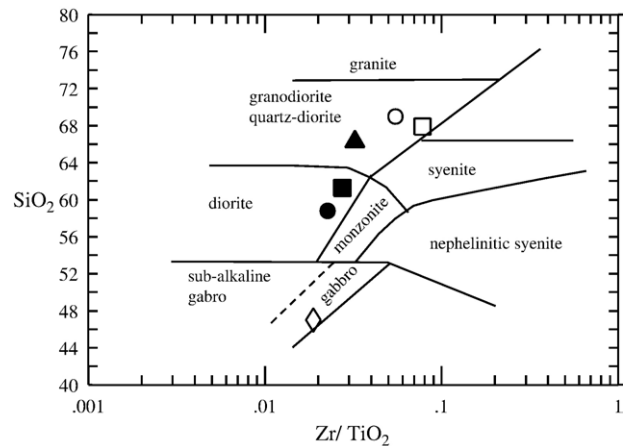


Fig. 8. SiO₂-Zr/TiO₂ diagram after Winchester and Floyd (1977) for Palimé-Amlamé granitoids. Southern area (Palimé) O ym22a, □ ym22c, ◇ ym33b. Northern area (Amlamé), ● ym47a, ■ ym67, ▲ Ezm.

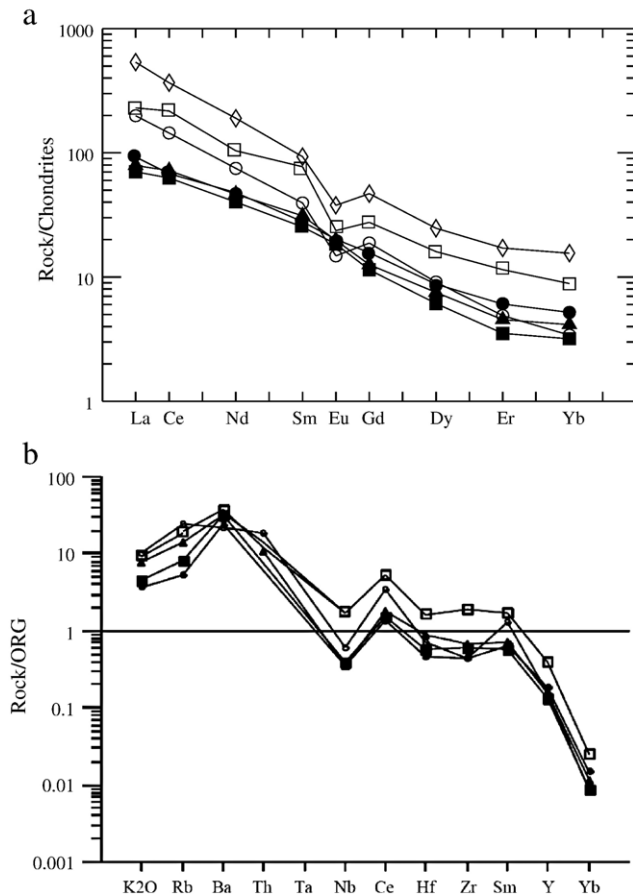


Fig. 9. a: Chondrite normalized (after Nakamura, 1974) REE plots for granitoids from Palimé–Amlamé. Symbols as Fig. 3. b: Trace-elements in granodiorites and diorites compared to Ocean Ridge Granites (ORG) after Pearce et al. (1984). Palimé area: ○ ym22a, □ ym22c, △ ym33b. Amlamé area: ● ym47a, ■ ym67, ▲ Ezm.

6.3. Isotopic data of Sm–Nd and Rb–Sr systems

Sm–Nd and Rb–Sr isotopic compositions are given in Table 4. The initial $^{87}\text{Sr}/^{86}\text{Sr}$ ratios of granitoids are close to mantle values at 2.17 Ga. $^{87}\text{Sr}/^{86}\text{Sr}$ ratios are higher in the monzogranite ym22a from Palimé (0.7031) than that from Amlamé (0.7019 to 0.7024) suggesting a more significant crustal component: i.e. larger crustal contribution to magma mixing processes or country rock assimilation as shown by numerous septa of migmatites. The mafic enclave ym33b shows the lowest $^{87}\text{Sr}/^{86}\text{Sr}$ value (0.701).

Table 4
Rb–Sr and Sm–Nd isotopic data

Sample	Rb	Sr	$^{87}\text{Rb}/^{86}\text{Sr}$	$^{87}\text{Sr}/^{86}\text{Sr}$	Error (2 σ)	$(^{87}\text{Sr}/^{86}\text{Sr})_i$	Sm (ppm)	Nd (ppm)	$^{147}\text{Sm}/^{144}\text{Nd}$	$^{143}\text{Nd}/^{144}\text{Nd}$	Error (2 σ)	$(\epsilon_{\text{Nd}})_i$	T_{DM} (in Ma) ($\epsilon_0 = +10$)	T_{DM} (in Ma) ($\epsilon_0 = +8$)
ym33b	79.1	827.6	0.28	0.709061	0.000010	0.7006	18.89	119.50	0.0955	0.511073	0.000018	(–2.9)	2664	2536
ym22a	100.4	431.8	0.67	0.723716	0.000012	0.7031	8.01	47.24	0.1025	0.511212	0.000009	(–2.1)	2642	2507
ym47a	24.8	764.1	0.09	0.705238	0.000012	0.7024	5.66	30.07	0.1138	0.511352	0.000006	(–2.4)	2728	2577
Ezm	57.4	660.0	0.25	0.709600	0.000012	0.7019	6.31	29.30	0.1302	0.511156	0.000006	(–10.8)	3608	3430

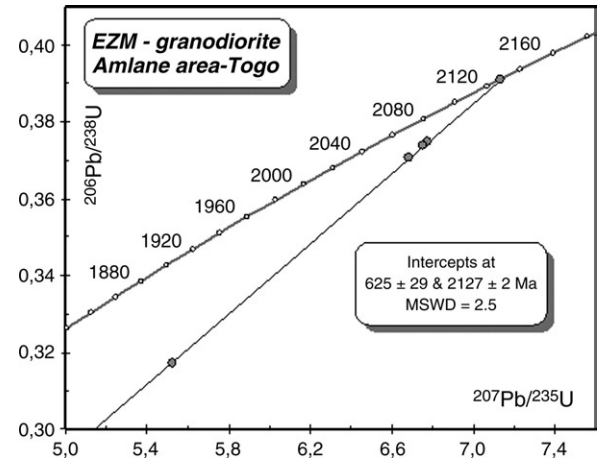


Fig. 10. U–Pb concordia diagram for the quartz–diorite (sample Ezm from the Amlamé area).

All the rocks, both granitoids and mafic enclave, display negative ϵ_{Nd} values at 2127 Ma implying their derivation from a crustal protolith, as previously suggested by the trace elements contents. Most of the set is characterized by homogeneous and slightly negative ϵ_{Nd} values (–2.1 to 2.9) with the striking exception of sample Ezm that shows a very negative signature (–11). Nd isotopes provide Nd T_{DM} model ages (Table 4) ranging between 2.64 and 2.72 Ga (or 2.51–2.58 using a less depleted mantle) for the former samples and 3.61 Ga (or 3.43) for the latter (Ezm). Such differences suggest a relative heterogeneity of the crustal precursors. Most of granitoids of the PAP may represent a mixing of different magmas deriving from Archaean continental crust and from depleted mantle at 2.1 Ga.

6.4. U–Pb geochronological data of the PAP

U–Pb zircons analyses were performed on a granodiorite of the Amlamé area (Ezm) at the isotopes geochemistry laboratory of the University of Clermond–Ferrand according to the method described in Paquette and Pin (2001). The analyzed zircon crystals were pink colored, euhedral, elongated (length/width ratio > 4) and very translucent. Five mechanically air-abraded fractions plot on a chord intersecting the Concordia at 2127 ± 2 Ma and 625 ± 29 Ma (Fig. 10 and Table 5). The upper intercept is interpreted as dating the crystallization of the PAP granitoids. The lower intercept at ca. 600 Ma is poorly defined,

Table 5
U–Pb isotopic data

Fraction	Weight (μg)	U Concentration (ppm)	Pb rad	$\frac{^{206}\text{Pb}^{(1)}}{^{204}\text{Pb}}$	$\frac{^{208}\text{Pb}^{(1)}}{^{206}\text{Pb}}$	Atomic ratios			Apparent ages (Ma)			Corresponding coefficients
				$\frac{^{206}\text{Pb}^{(2)}}{^{238}\text{U}}$	$\frac{^{207}\text{Pb}^{(2)}}{^{235}\text{U}}$	$\frac{^{207}\text{Pb}^{(2)}}{^{206}\text{Pb}^{(2)}}$	$\frac{^{206}\text{Pb}}{^{238}\text{U}}$	$\frac{^{207}\text{Pb}}{^{235}\text{U}}$	$\frac{^{207}\text{Pb}}{^{206}\text{Pb}}$			
1 > 150 μm [1] Ab	40	99	45.4	8225	0.2267	0.3911 (0.16)	7.1308 (0.18)	0.1323 (0.08)	2128	2128	2128	0.90
2 > 150 μm [6] Ab	80	134	59.3	3702	0.2319	0.3750 (0.12)	6.7732 (0.13)	0.1310 (0.04)	2053	2082	2112	0.95
3 > 150 μm [5] Ab	69	156	66.7	3137	0.1925	0.3739 (0.11)	6.7524 (0.12)	0.1310 (0.04)	2048	2080	2111	0.94
4 > 150 μm [7] Ab	80	150	65.5	3082	0.2292	0.3708 (0.12)	6.6842 (0.13)	0.1308 (0.04)	2033	2071	2108	0.96
5 > 150 μm [2] Ab	72	213	78.6	1052	0.1946	0.3172 (0.11)	5.5246 (0.12)	0.1263 (0.04)	1776	1904	2047	0.92

Individual analyses were performed on the least magnetic (2° forward and side tilt at 2.2 A using a Frantz Isodynamic magnetic barrier separator) crack-free zircon grains. The isotopic ratios are corrected for mass discrimination ($0.1 \pm 0.015\%$ per amu for Pb and U), isotopic tracer contribution and analytical blanks: 10 pg for Pb and less than 1 pg for U. Initial common Pb is determined for each fraction in using the Stacey and Kramers (1975) two-step model. Absolute errors in percent are given at the 2σ level, (1)=measured ratio; (2)=calculated ratio. Number in brackets is number of grains in fraction. Ab=zircon fraction mechanically abraded before dissolution (Krogh, 1982).

the calculated age and related error varying with the consideration or not of the fifth fraction. Consequently, a slight recrystallization responsible for the Pb loss of the zircon grains during the Pan-African metamorphism may be proposed, nevertheless, this dating does not allow a precise definition of the age of this event. Previous datings (Bernard-Griffiths et al., 1991; Attoh et al., 1997; Hirdes and Davis, 2002) suggested that the tectono-metamorphic events affecting the PAP granitoids could be close to ca. 600–590 Ma.

7. Discussion – conclusion

The PAP is built up by various granitoids (Fig. 3): monzogranites and quartz–monzonites, granodiorites, quartz–diorites and quartz–monzodiorites, that enclose gneisses and migmatitic gneiss septa together with mafic igneous enclaves. Field relationships between the mafic enclaves and their host granitoids testify for magma mixing and mingling (Fig. 2).

According to major, trace and REE elements, the PAP has geochemical affinities with calc-alkaline and TTG series. The calc-alkaline signature is also evidenced by the composition of igneous biotites (Fig. 4b). The metaluminous granitoids from the northern (Amlamé) and southern (Palimé) areas have medium to high-K character, respectively (Fig. 7). Relationships between granitoids from the northern (Qtz–monzodiorites, Qtz–diorites and granodiorites) and southern (Qtz–monzonites and monzogranites) PAP areas may be explained in terms of differentiation (Figs. 8 and 9), but a mixing process with a larger amount of crustal component cannot be ruled out.

As frequently reported, the mafic enclaves display a striking chemical convergence, even for isotopic signatures, with their host rocks, such homogenization arising from chemical diffusion during mixing and mingling processes between mantle and crust derived magmas (Fig. 9, Tables 3 and 4). Because of a restricted number of analyses, it would be difficult

to precisely define the mafic and silicic magma end-member compositions. The available data preclude any attempt to recognize the mantle source of the mafic enclaves as they appear to have been deeply modified by chemical exchange.

Different pressure values (6–8 kbar) and (4–6 kbar) were deduced from the chemistry of igneous amphiboles (tschermakitic hornblendes from mafic enclaves and magnesio-hornblende from Qtz–diorites and granodiorites, respectively). It is suggested that the mafic and intermediate magmas were equilibrated at different crustal levels before mingling and complete crystallization.

Clearly much more geochemical and geochronological data would be required to fully understand the precise tectonic and magmatic evolution of the Palimé–Amlamé granitoids. Nevertheless, such metaluminous granitoids showing striking affinities with transitional TTGs (Champion and Smithies, 2003; Moyen et al., 2003) that are thought to derive from both mantle peridotite and crustal, TTG like, sources. Moreover the Y depleted character, together with negative ϵ_{Nd} values, imply deep seated crustal sources with a large amount of garnet in the melt residue (Moyen et al., 2003; Jayananda et al., 2006).

It is well known that granitoids show a large compositional diversity because of the variety of their origins, sources, subsequent genesis and evolution processes, emplacement at different structural levels and under different tectonic regimes in distinct geodynamic environments (Pearce et al., 1984). However, the PAP granitoids, characterized by both mantle and crustal source and by high pressure conditions of melting, may be generated and emplaced in a thickened continental crust consistent with a post-collisional setting.

7.1. Regional significance of the PAP

The calc-alkaline pluton of Amlamé–Palimé is Paleoproterozoic in age (2127 ± 2 Ma), and this removes the remaining

ambiguity on its relationships with the Eburnean or the Pan-African orogenic processes. Many Paleoproterozoic intrusives have been reported in the western region of the Pan-African mobile belt in Ghana, Togo and Bénin. With respect to the Pan-African orogenic zonation (Caby, 1989; Affaton et al., 1991) these granitoids belong either to the active margin i.e. the Bénin–Nigerian shield or to the passive margin, i.e. the West African Craton. The former include the Mô complex in Bénin (2064 ± 90 Ma, Affaton et al., 1978; Caen-Vachette et al., 1979, Rb–Sr whole rock isochron); the Ibadan grey gneiss in Nigeria (2150 Ma, Grant, 1970, Rb–Sr whole rock and 2.7 Ga, Rahaman, 1988, U–Pb on zircon). Pan-African reworking commonly occurs as isotopic resetting of mineral (600 Ma, Rb–Sr on minerals, Grant et al., 1972) and local partial melting (Rahaman, 1988, U–Pb on zircon). On the other hand, many Paleoproterozoic granitoids appear as klippen and inliers on the western side of the main Pan-African suture and consist of basement nappes closely associated with Pan-African metasedimentary rocks and mafic to ultramafic meta-igneous rocks. These western granitoids have been recognized in SE Ghana (Hô gneisses, 2176 ± 44 Ma, Rb–Sr whole rock isochron, Agyei et al., 1987), in N Togo (Kara orthogneiss, 2077 ± 62 Ma, Rb–Sr whole rock isochron, Caen-Vachette et al., 1979) and SE Mali (Bourré metagranitoids, 2080 Ma, U–Pb zircon, La Boisse and Lancelot, 1977; Caby and Moussine-Pouchkine, 1978). All the granitoids from the passive margin have been extensively recrystallized to orthogneiss and they present both isotopic resetting and tectonic and metamorphic features of Pan-African age (Kara, 608 ± 17 Ma, Rb–Sr mineral, Caen-Vachette et al., 1979; Hô gneiss, 579 ± 0.4 Ma, $^{40}\text{Ar}/^{39}\text{Ar}$, Attoh et al., 1997).

In that framework, the PAP may clearly be attached to the WAC passive margin: it outcrops as a window under west vergent nappes including various lithologies (high grade and low grade metasedimentary rocks, eclogites and ultramafics) derived from the Pan-African accretionary wedge (Ménot and Seddoh, 1977, 1985; Agbossoumondé et al., 2001; Attoh and Morgan, 2004), and granulites and gneisses arising from continental arc assemblage (Agbossoumondé et al., 2004; Duclaux et al., 2006). Moreover, the post-solidus tectonic and metamorphic imprint is clearly related to the Pan-African history (625 ± 29 Ma) and is consistent with the structures and P – T conditions of the Pan-African country rocks.

7.2. Conclusions

We conducted fieldwork and collected samples of granitoids in the Palimé–Amlamé area, and carried out reconnaissance whole-rock chemical analyses in order to evaluate their chemical characteristics and possible regional tectonic setting. In addition, we have obtained a new U–Pb zircon age for the Amlamé granodiorite, which places new constraints on regional correlations and tectono-thermal activity in the Dahomeyide Pan-African belt. The following conclusions may be drawn from the results of this study:

i) Granitoids from the PAP represent various facies from a calc-alkaline magnesian series. They exhibit clear field,

mineralogical and chemical evidence of magma mixing and mingling mechanisms between mafic and silicic magmas. The crustal component derives from partial melting of an Archaean (2.5 to 3.6 Ga) lower crust and formed metaluminous, I-Type granitoids, but the juvenile (2.1 Ga) mantle component cannot be constrained. The PAP may have crystallized in a post-collisional tectonic setting.

ii) A 2127 ± 2 Ma age (U–Pb zircon) dates crystallization of the PAP, which is clearly related to the Eburnean orogen and was emplaced within the present day West African Craton. Moreover it was later involved in the Pan-African collision as marked out by the lower intercept age at 625 ± 29 Ma.

The PAP clearly represents a fragment (basement nappe or parautochthonous unit?) of the eastern margin of the WAC strongly reworked during the amalgamation of Western Gondwana.

Acknowledgements

This research was supported by the University of Saint Etienne, UMR CNRS 6524 for analytical resources and by the University of Lomé for logistics. This work was partly granted by AUF (Agence Universitaire de la Francophonie) for a joint-research between Universities of Lomé, Abomey-Calavi, Saint-Etienne and Lyon (project PCSI 6313 PS437). We greatly acknowledge the constructive reviews of Jean Jacques Peucat (Rennes) and Renaud Caby (Montpellier) which substantially helped to improve this paper.

Appendix A. Analytic techniques

Mineral compositions were determined with a CAMECA SX 100 microprobe at University Blaise Pascal (Clermont–Ferrand) UMR CNRS 6524. The analytical conditions were 15 kV, 10 nA for a counting time of 10 s. Natural minerals were used as standards.

Major elements contents (except Rare Earth Elements, REE) were analyzed by standard X-ray fluorescence. Trace elements and REE were analyzed by ICP-ES at CRPG-Nancy.

Nd and Sm were separated using wet chemical chromatographic methods, ultra-pure acids and conventional cation specific separation resins at University of Saint Etienne, UMR CNRS 6524. Isotopic ratios were determined by thermal ionization mass spectrometry at University Blaise Pascal (Clermont–Ferrand) UMR CNRS 6524. The reproducibility of the Sr standard (NBS 987) is $^{87}\text{Sr}/^{86}\text{Sr}$: 0.710269 ± 0.000011 and of the Nd standard (AMES) is $^{143}\text{Nd}/^{144}\text{Nd}$: 0.511977 ± 0.000007 . Typical analytical errors in the $^{87}\text{Rb}/^{86}\text{Sr}$ and $^{147}\text{Sm}/^{144}\text{Nd}$ ratios are better than 0.1%. Time corrected, Nd values are calculated using a present-day CHUR (Chondritic Uniform Reservoir) composition of $^{143}\text{Nd}/^{144}\text{Nd}$: 0.51264. The T_{DM} models ages were calculated using values for the present-day depleted mantle of 0.51351 ($\epsilon_0 = +10$) and 0.51305 ($\epsilon_0 = +8$) and assuming a radiogenic linear growth for the mantle starting at 4.54 Ga.

References

- Affaton, P., Sougy, J., Trompette, R., 1978. The tectono-stratigraphic relationship between the Upper Precambrian and Lower Paleozoic Volta basin and the Pan-African Dahomeyide orogenic belt (West Africa). *American Journal of Science* 280, 224–248.
- Affaton, P., 1990. Le bassin des Volta (Afrique de l'Ouest): une marge passive du Protérozoïque supérieur, tectonisé au Panafricain (600+/-50 Ma). Thèse Doctorat d'Etat, 2 vol., Collection Etudes et Thèses, Ed. ORSTOM, Paris, 499p.
- Affaton, P., Rahaman, M.A., Trompette, R., Sougy, J., 1991. The Dahomeyide Orogen: Tectonothermal Evolution and Relationships with the Volta Basin. In: Dallmeyer, R.D., Lecorche, J.P. (Eds.), *The West African Orogens and Circum-Atlantic Correlatives*. Springer-Verlag, Berlin, pp. 107–122.
- Agbossoumondé, Y., Ménot, R.P., Guillot, S., 2001. Metamorphic evolution of Neoproterozoic eclogites from South Togo (West Africa). *Journal of African Earth Sciences* 33 (2), 227–244.
- Agbossoumondé, Y., Guillot, S., Ménot, R.P., 2004. Pan-African subduction–collision event evidenced by high-P coronas in metanorites from the Agou massif (Southern Togo). *Precambrian Research* 135 (1/2), 1–21.
- Agevi, E.K., van Landewijk, J.E.J.M., Armstrong, R.L., Harakal, J.E., Scott, K.L., 1987. Rb–Sr and K–Ar geochronometry of southeastern Ghana. *Journal of African Earth Sciences* 6, 153–161.
- Anderson, B., Smith, R., 1995. The effects of temperature and fO_2 on the Al-hornblende barometer. *American Mineralogist* 80, 549–559.
- Attoh, K., 1990. Dahomeyides in southern Ghana: evidence for oceanic closure and crustal imbrication in a Pan-African, orogen. *Memoire C.I.F.E.G.* 22, 159–164.
- Attoh, K., Morgan, J., 2004. Geochemistry of high-P granulites from the Pan-African Dahomeyide orogen, West Africa: constraints of the origin and composition of the lower crust. *Journal of African Earth Sciences* 39 (3/5), 201–208.
- Attoh, K., Dallmeyer, R.D., Affaton, P., 1997. Chronology of nappe assembly in the Pan-African Dahomeyide orogen, West Africa: evidence from $^{40}\text{Ar}/^{39}\text{Ar}$ minerals age. *Precambrian Research* 82, 153–171.
- Barbarin, B., 1996. Genesis of the two main types of peraluminous granitoids. *Geology* 24, 295–298.
- Barbarin, B., 1999. A review of the relationships between granitoid types, their origins and their geodynamic environments. *Lithos* 46, 605–626.
- Barbarin, B., 2004. Mafic magmatic enclaves and mafic rocks associated with some granitoids of the central Nevada batholith, California: nature, origin, and relations with the hosts. *Lithos* 80, 155–177.
- Bernard-Griffiths, J., Peucat, J.J., Ménot, R.P., 1991. Isotopic (Rb–Sr, U–Pb and Sm–Nd) and trace element geochemistry of eclogites from the Pan-African belt: a case study from REE fractionation during high-grade metamorphism. *Lithos* 27, 43–57.
- Caby, R., 1987. The Pan-African belt of West Africa from the Sahara to the Gulf of Benin. In: Rodgers, J., Schaer, E.J.P. (Eds.), “The anatomy of mountains range”. Princeton Univ. Press, pp. 129–170.
- Caby, R., 1989. Precambrian terranes of Benin–Nigeria and Northeast Brazil and the Late Proterozoic South Atlantic fit. *Geological Society of America Special Paper* 230, 145–158.
- Caby, R., Moussine-Pouchkine, A., 1978. Le horst birrimien de Bourré (Gourma oriental, République du Mali): nature et comportement au cours de l'orogénèse pan-africaine. *Comptes Rendus de l'Académie des Sciences, Paris* 287, 5–8.
- Caen-Vachette, M., Pinto, J.M., Roques, M., 1979. Plutons éburnéens et métamorphisme dans le socle cristallin de la chaîne Pan-Africaine au Togo et au Bénin. *Revue Géographie Physique et Géologie Dynamique* 21, 351–357.
- Castaing, C., Aregba, A., Assih-Edeou, P., Chevremont, P., Godonou, K.S., Sylvain, J.P., 1988. Les unités gneissiques et la zone de cisaillement crustal du Sud-Togo. *Journal of African Earth Sciences* 7 (5/6), 821–828.
- Champion, D.C., Smithies, R.H., 2001. Archaean granites of the Yilgarn and Pilbara cratons, Western Australia. In: Cassidy, K.F., Dunphy, J.M., Van Kranendonk, M.J. (Eds.), *Proceedings of the Fourth International Achaean Symposium*. Perth, Australia, pp. 134–136. AGSO-Geoscience Australia, record 2001/37.
- Champion, D.C., Smithies, R.H., 2003. Archaean granites. In: Blevin, P.L., Chappell, B.W., Jones, M. (Eds.), *Magma to Mineralisation: The Ishihara Symposium*, (AGSO-Geoscience Australia, record 2003/14), pp. 19–24.
- Chappell, B.W., White, A.J.R., 1992. I and S-type granites in the Lachlan Fold Belt. *Transactions of the Royal Society of Edinburgh. Earth Sciences* 83, 1–26.
- Clarke, D.B., 1992. *Granitoid Rocks*, Topics in the Earth Sciences, vol. 7. Chapman and Hall, London. 283p.
- Defant, M.J., Drummond, M.S., 1990. Derivation of some modern arc magmas by melting of young subducted lithosphere. *Nature* 347, 662–665.
- Didier, J., Barbarin, B., 1991. The different types of enclaves in granites. Nomenclature, Enclaves and Granite Petrology. In: Didier, J., Barbarin, B. (Eds.), *Developments in Petrology*, vol. 3. Elsevier Amsterdam, pp. 19–23.
- Duclaux, G., Ménot, R.P., Guillot, S., Agbossoumondé, Y., Hilairet, N., 2006. The mafic layered complex of the Kabyé massif (north Togo and north Bénin): evidence of a Pan-African granulitic continental arc root. *Precambrian Research* 151, 101–118.
- Ferré, E.C., Leake, B.E., 2001. Geodynamic significance of early orogenic high-K crustal and mantle melts: example of the Corsica batholith. *Lithos* 59, 47–67.
- Frost, B.R., Barnes, C.G., Collins, W.J., Arculus, R.J., Ellis, E.J., Frost, C.D., 2001. A geochemical classification for granitic rocks. *Journal of Petrology* 42 (11), 2033–2048.
- Grant, N.K., 1970. Geochronology of Precambrian basement rocks from Ibadan, SW Nigeria. *Earth and Planetary Science Letters* 10, 29–38.
- Grant, N.K., Hickman, M.H., Burkholder, F.R., Powell, J.L., 1972. Kibaran metamorphic belt in Pan-African domain of West Africa? *Nature* 238, 90–91.
- Hirdes, W., Davis, D.W., 2002. U–Pb zircon and rutile metamorphic ages of Dahomeyan garnet–hornblende gneiss in southeastern Ghana, West Africa. *Journal of African Earth Sciences* 35, 445–449.
- Jayananda, M., Chardon, D., Peucat, J.-J., Capdevila, R., 2006. 2.61 Ga potassic granites and crustal reworking in the western Dharwar craton, southern India: tectonic, geochronologic and geochemical constraints. *Precambrian Research* 150.
- La Boisse, De H., Lancelot, J.R., 1977. A propos de l'événement à 1000 Ma en Afrique occidentale: 1. Le « granite » de Bourré. *Comptes Rendus sommaires de la Société Géologique de France* 4, 223–225.
- Leake, B.E., 1990. Granites magmas: their sources, initiation and consequences of emplacement. *Journal of the Geological Society (London)* 147, 579–589.
- Leake, B.E., Woolley, A.R., Arps, C.E.S., Birch, W.D., Gilbert, M.C., Grice, G.D., Hawthorne, F.C., Kato, A., Kisch, H.J., Krivovichev, V.G., Linthout, K., Laird, J., Mandarino, J.A., Maresch, W.V., Nickel, E.H., Rock, N.M.S., Schumacher, J.C., Smith, D.C., 1997. Nomenclature of amphiboles. Report of the Subcommittee on amphiboles of the Intern. Mineral. Assoc. Comm. on new minerals and names. *American Mineralogist*, vol. 82, pp. 1019–1037.
- Le Maître, R.W., 1989. A classification of igneous rocks and glossary of terms. Blackwell scientific publications, Oxford. 193p.
- Maniard, R.D., Piccolli, P.M., 1989. Tectonic discrimination of granitoids. *Geological Society of America Bulletin* 101, 635–643.
- Martin, H., 1999. Adakitic magmas: modern analogues of Archaean granitoids. *Lithos* 46, 411–429.
- Ménot, R.-P., 1980. Les massifs basiques et ultrabasiques de la zone mobile panafricaine au Ghana, Togo et au Bénin. Etat de la question. *Bulletin de la Société Géologique de France* 7, 297–303.
- Ménot, R.P., Seddo, K.F., 1977. Données nouvelles sur la pétrographie de l'Atacorien au Togo (Région des Plateaux, Atakpamé). *Bulletin de la Société Géologique de France* 7, 331–334.
- Ménot, R.P., Seddo, K.F., 1985. The eclogites of Lato Hills (South Togo, West Africa): relics from early tectonometamorphic evolution of the Pan-African orogeny. *Chemical Geology* 50, 313–330.
- Moyen, J.-F., Martin, H., Jayananda, M., Auvray, B., 2003. Late Archaean granites: a typology based on the Dharwar Craton (India). *Precambrian Research* 127, 103–123.
- Nakamura, N., 1974. Determination of REE, Ba, Mg, Na and K in carbonaceous and ordinary chondrites. *Geochimica et Cosmochimica Acta* 38, 757–775.
- Otten, M.T., 1984. The origin of brown hornblende in the Artjället gabbros and dolerites. *Contributions to Mineralogy and Petrology* 86, 189–199.

- Paquette, J.L., Pin, C., 2001. A new miniaturized extraction chromatography method for precise U–Pb zircon geochronology. *Chemical Geology* 176, 313–321.
- Pearce, J.A., 1996. Sources and setting of granitic rocks. *Episodes* 19, 120–125.
- Pearce, J.A., Harris, N.B.W., Tindle, A.G., 1984. Trace elements discrimination diagrams for the tectonic interpretation of granitic rocks. *Journal of Petrology* 25, 956–983.
- Rahaman, M.A., 1988. Recent advances in the study of the basement complex of Nigeria. In: Oluyide, P., et al. (Ed.), *Precambrian geology of Nigeria*. Geological Survey of Nigeria, pp. 11–43.
- Rickwood, P.C., 1989. Boundary lines within petrologic diagrams which use oxides of major and minor elements. *Lithos* 22, 247–263.
- Rottura, A., Del Moro, A., Caggianelli, A., Bargossi, G.M., Gasparotto, G., 1997. Petrogenesis of the Monte Croce granitoids in the context of the Permian magmatism of Southern Alps, Italy. *European Journal of Mineralogy* 9, 1293–1310.
- Schmidt, M.W., 1992. Amphibole composition in tonalite as function of pressure. An experimental calibration of the aluminium in hornblende. *Contributions to Mineralogy and Petrology* 110, 304–310.
- Streckeisen, A., Le Maître, R.W., 1979. A chemical approximation to the modal QAPF classification of the igneous rocks. *Neues Jahrbuch für Mineralogie Abhandlungen* 136, 169–206.
- Sylvain, J.P., Aregba, A., Assih-Edeou, P., Castaing, C., Chevremont, Ph., Collart, J., Monciardini, C., Marteau, P., Ouassane, I., Tchota, A., 1986. Notice explicative de la carte géologique à 1/200000 du Togo, feuilles Lomé et Atakpamé. D.G.M.G./B.N.R.M., Lomé, Togo.
- Tarney, J., Jones, G.E., 1994. Trace element geochemistry of orogenic igneous rocks and crustal growth models. *Journal of the Geological Society of London* 151, 855–868.
- Tindle, A.G., 1991. Trace element behaviour in microgranular enclaves from granitic rocks. In: Didier, J., Barbarin, B. (Eds.), “Enclaves and granite petrology”. Elsevier, Amsterdam, pp. 313–331.
- Trompette, R., 2000. Gondwana evolution; its assembly at around 600 Ma. *Comptes Rendus de l’Académie des Sciences, Paris* 330, 305–315.
- Winchester, J.A., Floyd, P.A., 1977. Geochemical discrimination of different magma series and their differentiation products using immobile elements. *Chemical Geology* 20, 325–343.